A spring poleward current and its influence on microplankton assemblages and harmful dinoflagellates on the western Iberian coast

B.G. Crespo* and F.G. Figueiras

Instituto de Investigacións Mariñas, CSIC, Eduardo Cabello 6, E-36208 Vigo, Spain

* Corresponding author. Tel.: +34986 231930; fax: +34986 292762

E-mail address: bibiana@iim.csic.es (B.G. Crespo)

Abstract

Along-shore currents can propagate Harmful Algal Blooms (HABs) over long distances in many coastal areas of the ocean. Harmful dinoflagellate blooms on the west coast of Iberia frequently occur when the Iberian Poleward Current (IPC) establishes on the continental slope. This has led to the suggestion that HABs could be transported northward by the IPC. To examine this possibility, the microplankton composition along the west coast of Iberia was studied in May 1993 coinciding with the presence of the IPC. The microplankton of the IPC was almost exclusively composed of small flagellates, with the notable absence of the harmful species usually associated with coastal waters. The primary influence of the IPC was to confine coastal microplankton populations to the shelf, where a downwelling convergence prevented their export from the coastal environment. Microplankton assemblages on the shelf revealed a north-south gradient related to different stages of succession. Earlier stages of succession in which diatoms were prominent were found on the northern shelf, whereas dinoflagellates were more abundant in the south. The toxic species Gymnodinium catenatum, which was only present in the southern shelf, did not show a northward transport associated with the IPC. It is suggested that the northward spreading of HABs along the west coast of Iberia must be related to the interaction between the IPC, which accumulates coastal populations on the shelf, and the latitudinal progress of microplankton succession that determines species composition. Thus, during the course of the season, HABs are likely to be observed in the south prior to their development in the north.

Keywords: microplankton distribution, spring poleward flow, harmful algal blooms, Gymnodinium catenatum, accumulation, Iberian upwelling.

1. Introduction

Harmful Algal Blooms (HABs) impact many coastal areas of the world ocean (GEOHAB, 2001) where they may have severe economic and ecological consequences (Smayda, 1990; Anderson et al., 2002) and often induce human illness. For these reasons, there is constant research focused on understanding which factors trigger, maintain and propagate these blooms along the coastlines. Although this research has revealed that HABs result from a complex interaction among physical, chemical and biological factors that operate at different rates and several spatial and temporal scales, it is evident now that along-shore and across-shelf currents play a key role in HAB dynamics in many coastal areas. Thus, blooms generated in offshore waters may be advected to the coast by onshore currents (Tester and Steidinger, 1997; Raine and McMahon, 1998; Anderson et al., 2005), while alongshore flows can transport HABs hundreds of kilometres along the coast (Tester et al., 1991; Franks and Anderson, 1992). Frequently, these two currents combine to first concentrate and/or advect blooms towards the coast and next disseminate them (Tester et al., 1991; Anderson et al., 2005). This kind of combination has been reported as especially important in coastal upwelling systems (Pitcher and Boyd, 1996; Pitcher et al., 1998; Trainer et al., 2002), where across-shelf and along-shore currents are prominent physical features. In addition to the transport of HABs, it has also been suggested that alongshore and onshore currents may interact to create suitable environmental conditions for the *in situ* development of HABs (Figueiras et al., 1998; Ryan et al., 2005). To establish the extent to which the transport of populations *versus* the modification of environmental conditions influence HAB dynamics within a specific region is important in developing accurate models of blooms and in managing HABs.

The general circulation in the western Iberian margin, a region where HABs of dinoflagellates are recurrent (e.g. Margalef, 1956; Fraga et al., 1988; Figueiras et al., 1994; Moita et al., 1998), is greatly influenced by seasonal upwelling-downwelling (Wooster et al., 1976). In summer, dominant northeasterly winds cause upwelling on the shelf and a surface southward flow near the shelf break (Ambar and Fiúza, 1994). The predominance of southwesterly winds during winter strengthens the general circulation of the region, which is characterised by the presence of a surface poleward current on the slope (Frouin et al., 1990; Haynes and Barton, 1990; Álvarez-Salgado et al., 2003; Peliz et al., 2005; Torres and Barton, 2006) that forces an associated shoreward flow at the surface and induces coastal downwelling (Castro et al., 1997; Álvarez-Salgado et al., 2003). This Iberian Poleward Current (IPC) originates at approximately 39-40ºN from an intrusion of subtropical oceanic water that flows along western and northern Iberia to reach the Armorican Shelf off SW France (Pingree and Le Cann, 1990) and even the Goban Spur region near 50ºN (Pingree et al., 1999). HABs of dinoflagellates on the western Iberian coast often succeed the development of the IPC (e.g. Fraga et al., 1988, 1993; Estrada, 1995). Furthermore, toxic episodes in the north frequently occur a few days after they are detected in the south. Although these observations have led to suggest that HABs on the northern coast result from their transport from the south (Sordo et al., 2001), direct evidence remains to be established.

Here we report on how the IPC affects the microplankton distribution in the western Iberian margin in spring. We thereby assess the role that the IPC has in the northward transport of HABs or in the modification of the environment to create suitable conditions for the development of HABs.

2. Material and methods

2. 1. Study area and sampling

The western Iberian margin was extensively sampled at 92 stations in the spring of 1993 (12-26 May) on board of the RV "Cornide de Saavedra". The stations, located along 13 sections perpendicular to the shoreline between 9º and 11ºW and from 40º to 43ºN (Fig. 1a), were initially surveyed using a conductivity-temperature-depth (CTD) equipped with a fluorometer and a rosette with PVC Niskin bottles. Sampling began at the northernmost section 1 and ended at section 13 in the south. Nitrate and chlorophyll *a* concentrations and microplankton abundance were determined at several depths from surface to the bottom in shelf waters and from surface to 100-150m deep in the open ocean stations. Water samples were collected from the CTD upcasts.

2. 2. Ekman transport components

The magnitude and direction of the wind in front of Cape Finisterre (43º N, 11º W) deduced from surface pressure charts were used to calculate cross-shelf (Qx) and along-shore (Qy) Ekman transport components ($m^3\ s^{-1}\ km^{-1}$) according to Wooster et al. (1976):

$$Q_{X,Y} = \frac{\rho_{air} C_D |V| V_{Y,X}}{\rho_{sw} f}$$

where ρ_{air} is the air density (1.22 kg m^{-3}), C_D is the empirical drag coefficient (1.3 x 10^{-3}, dimensionless) according to Hidy (1972), $|V|$ is the wind speed at the sea surface with components $V_{Y,X}$, ρ_{sw} is the seawater density (~1025 kg m^{-3}) and f is the Coriolis parameter at 43º N (9.946 x 10^{-5} s^{-1}). Since SW winds force northward and

119 onshore (downwelling) transport and NE winds cause southward and offshore
120 (upwelling) transport, the sign of Qx was changed to facilitate comparisons between
121 both transport components. Therefore, positive and negative values (Fig. 1b) indicate
122 southward-upwelling and northward-downwelling transport, respectively.
123
124 *2. 3. Nitrate, chlorophyll a and microplankton*
125 Nitrate concentrations (µmol kg^{-1}) were determined using a segmented flow analysis
126 system, Technicon AAII, by the reduction method to nitrite (Hansen and Grassoff,
127 1983) with some modifications (Mouriño and Fraga, 1985).
128 Chlorophyll *a* (chl *a*; mg m^{-3}) was determined by fluorometry using a Turner Designs
129 fluorometer calibrated with pure chlorophyll *a* (Sigma Chemical Co.). Seawater
130 samples of 100 ml were filtered under low vacuum pressure through 25 mm Whatman
131 GF/F filters, which were immediately frozen at -20ºC. Pigments were extracted in 90 %
132 acetone over 24 h in the dark at 4ºC.
133 Microplankton samples of 100 ml were preserved in Lugol's iodine and sedimented
134 in composite sedimentation chambers. The organisms were counted and identified to
135 species level, when possible, using an inverted microscope. The small species (<20 µm)
136 were counted from two transects at x400 and x250 magnifications and the large species,
137 typically less abundant, were counted from the whole slide at x100 magnification.
138 Inverted microscope counts do not include the picoplankton fraction (<2 µm) and the
139 preservation procedure may cause losses in the nanoplankton fraction (2-20 µm), which
140 is mainly composed of flagellates.
141 Principal component analysis (PCA) was used to reduce and simplify the information
142 included in the list of species abundance, to resolve changes in species composition and
143 to identify assemblages within the microplankton community. The analysis was carried

144 out with the correlation matrix of species abundances transformed to log (X + 1), where
145 X is the number of cells per 100 ml. Since double zero values in the correlation matrix
146 can distort the results, these were reduced by including in the analysis only those
147 species present in at least 20 % of the samples. This provided an initial matrix of 41
148 species and 449 samples.
149
150 **3. Results**
151 *3. 1. Wind pattern and hydrographic field*
152 Sampling, which took place under downwelling conditions (Fig. 1b), was preceded
153 by an upwelling event that relaxed at the beginning of the sampling period (12-15 May).
154 Then, intense and highly variable southwesterly winds caused a strong downwelling (-
155 Qx = - 922 ± 952 $m^3 s^{-1} km^{-1}$; Qy = -457 ± 399 $m^3 s^{-1} km^{-1}$) that persisted until after the
156 cruise.
157 Although poorly defined by surface temperature (Fig. 2a), the IPC was clearly visible
158 from surface salinity (Fig. 2b), where it can be traced by salinities > 35.9. The IPC,
159 which developed a strong salinity gradient over the shelf where the less saline coastal
160 waters were confined, was characterised by a wide tongue of salty water (S >35.9) south
161 of 42ºN that became narrower to the north (Fig. 2b). The vertical sections of salinity
162 (Figs. 3f-j) show that the core of the IPC was deeper (~150m) and saltier (S = 36.0) in
163 the south than in the north, where the core of the IPC surfaced near the coast. The
164 vertical sections also indicate that the main intrusion of the saline water from the ocean
165 occurred as a surface layer of ~150 m at about 41-42 ºN (section 6, Fig. 3h). The
166 downward orientation of the isotherms and isohalines towards the coast (Figs. 3a-j)
167 indicates that the IPC induced downwelling at the shelf break, due to its confluence with

surface coastal waters with higher continental influence. The counterpart to this downwelling was a divergence at the ocean side (Figs. 3a-j).

3. 2. Nitrate and chlorophyll

While surface waters in the IPC and shelf domain showed nitrate depletion (< 0.05 μmol kg^{-1}), low nitrate concentrations (0.1-0.8 μmol kg^{-1}) were detected at the oceanic stations in the NW corner of the sampling area (Fig. 2c). This was caused by the divergent front on the oceanic side of the IPC, which induced a shallowing of the nitracline (Fig. 4b). The depth of the nitracline, modulated by the convergence at the shelf break and the divergence on the oceanic side of the IPC (Figs. 4a-e), was therefore shallower in the north than in the south, consistent with the surfacing of the IPC in the north (Figs. 3f-j) and weaker downwelling at the start of sampling when the northern sections were visited.

Chl *a* concentrations in the surface waters were generally low (Fig. 2d), with a subsurface chlorophyll maximum (Figs. 4f-j) associated with the nitracline (Figs. 4a-e). Consequently, the chlorophyll maximum surfaced (Figs. 2d, 4f-g) where the nitracline was shallower (Figs. 2c, 4b). Thus, the highest chl *a* values in the surface layer were recorded in the NW corner, where the highest surface nitrate concentrations were also measured (Fig. 2c). Coastal surface waters in the NE, off the Rías Baixas, had the lowest chl *a* concentrations (~0.2 mg chl *a* m^{-3}) owing to downwelling on the shelf induced by the IPC (Figs. 3f-g) that impeded surfacing of the chlorophyll maximum (Figs. 4f-g). In contrast, the subsurface chlorophyll maximum showed a slight surfacing in the SE (Figs. 4h-j) and, therefore, shelf surface waters south of the Rías Baixas had chl *a* values somewhat higher than those of the surface waters of the IPC (Fig. 2d).

193 *3. 3. Microplankton abundance and distribution*

194 Small flagellates dominated the microplankton community accounting for 75% of
195 the total cell abundance. Dinoflagellates and diatoms represented 18% and 5%,
196 respectively, while ciliates accounted for the remaining 2%. In general, cell abundance
197 was lower in the IPC than in the surrounding waters (Fig. 5a).

198 Diatoms, which were absent from the IPC waters, were mainly confined to the coast
199 (Figs. 5b, 6a-e), although they were also present in the surface waters of the oceanic
200 stations in the NW corner, outside of the IPC domain (Figs.5b, 6a-b). Coastal surface
201 waters showed higher diatom abundance in the north, outside of the Rías Baixas, than in
202 the south (Fig. 5b). In the south, diatoms were mostly found in subsurface waters (Figs.
203 6d, e). The most abundant species in shelf waters were small centric diatoms,
204 Leptocylindrus spp., Pseudo-nitszchia cf. seriata and Chaetoceros curvisetus.
205 Phaeodactylum tricornutum and small centric diatoms dominated the diatom community
206 in the NW. The northernmost section (section 1, Fig. 6a) showed the maximum diatom
207 abundance in shelf waters at around 100 m depth, while the oceanic maximum was
208 located in surface waters. In section 3 (Fig. 6b) the distribution suggests the upward
209 advection of diatoms at station 17.

210 The dinoflagellate community was dominated by small species such as
211 Prorocentrum minimum, small Gymnodinium spp., Heterocapsa niei, and Amphidinium
212 flagellans, which accounted for 81% of the total dinoflagellate abundance. The
213 contribution of small species to the dinoflagellate community was even higher in the
214 IPC (92%) and in the chlorophyll maximum located in the NW corner (94%) (Figs. 5c,
215 6f). Small dinoflagellates were somewhat less important (77%) in the other
216 dinoflagellate maximum located in the SE (Figs. 5c, 6j). At this location, where
217 Heterocapsa niei accounted for 42% of the total dinoflagellate abundance, the large

dinoflagellate Gymnodinium catenatum attained a significant proportion, representing 15% of total dinoflagellates and 74% of the total abundance of larger dinoflagellates.

Small flagellates, though ubiquitous (Fig. 5d), showed two zones of maximum abundance. One was in the surface waters of the IPC in the north (Figs. 5d, 6l), where abundances >500 cells ml^{-1} contributed to the surface chlorophyll maximum found in this area (Figs. 2d, 4g). The other maximum (>400 cells ml^{-1}) was in the subsurface waters (~35m) corresponding to the main entry of oceanic waters to form the IPC (section 6, Fig. 6m). In both cases small flagellates accounted for >90% of the total microplankton abundance. Small flagellates were the most important components of the microplankton community in the IPC (75%), in which small dinoflagellates accounted for 19%, and diatoms, large dinoflagellates and ciliates represented 2% each.

3. 4. Microplankton assemblages

PCA analysis extracted three principal components that explained 35 % of the total variance in the original data set of microplankton abundance. The first principal component (PC1) explained 18 %, the second (PC2) explained 10 % and the third (PC3) explained 7 %. The dinoflagellate Cystodinium steini was the only species that showed a small negative load with PC1 (Table 1). The load arrangement of the species with this component, with almost all species having positive loads, and the positive correlation (r = 0.68) between the logarithm of total cell abundance and the PC1 scores (not shown) indicate that PC1 explained the variance due to variations in cell abundance (Fig. 5a).

The large dinoflagellates Gyrodinium spirale and Gymnodinium catenatum, the diatom Proboscia alata and the flagellate Solenica setigera showed the highest positive loads (>0.4) with PC2 (Table 1). Cryptophyceae spp., small flagellates, 3 ciliates (Strombidium turbo, Strombidium strobilum and Strombidium conicum), and several

small Gymnodinium species had the highest negative loads (<-0.4). The distributions of the PC2 scores showed positive values in the SE, with the rest of the sampling area to be occupied by negative scores (Figs. 7a, 8d-e). The highest negative values were located in the main body of the IPC and in the NW corner (Figs. 7a, 8a-c).

PC3 differentiated between an assemblage composed of diatoms (Leptocylindrus danicus, small centric diatoms, Pseudo-nitzschia *cf.* seriata) and ciliates (Strobilidium spiralis and Mesodinium rubrum) with positive loads >0.4, and another assemblage of large dinoflagellates (dominated by Lingulodinium polyedrum and Ceratium furca) with negative loads <-0.4 (Table 1). The surface distribution of the PC3 scores (Fig. 7b) showed positive values on the shelf, except in the south where the highest negative scores were found. Also the IPC and the ocean stations in the NW had negative scores. Figure 8 shows that the negative scores were mainly found in the southern sections (sections 6 to 12; Figs. 8h-j). Lower negative scores in the northern part were restricted to the surface layer of the most oceanic stations and to the entire water column in the middle of the sections (sections 1 and 3; Figs. 8f, g). Southern shelf waters had positive scores of PC3 in the bottom layers (Fig. 8j).

3. 5. The distribution of Gymnodinium catenatum

The presence in the region of the toxic dinoflagellate Gymnodinium catenatum, which often causes severe HABs in the Rías Baixas on the northern coast (Fraga et al. 1988, Figueiras & Pazos 1991, Figueiras et al. 1994, Fermín et al. 1996), led us to examine its distribution. This species was restricted to shelf waters in the SE (Fig. 9a), outside of the IPC, with the highest abundances at about 50 m (Figs. 9b, c). There were no records of G. catenatum northward of 41ºN.

4. Discussion

The IPC reported here follows the scheme proposed by Peliz et al. (2005) in their review of the IPC regime, according to which the poleward flow in the western Iberian margin originates as an eastward advection of relatively warm salty water at about 39-40 ºN that shifts northward near the continental shelf to generate the IPC. Its formation, which is related to the large scale meridional density gradients in the NE Atlantic (Frouin et al., 1990; Pingree et al., 1999; Peliz et al., 2005), is also greatly favoured by southerly winds (Frouin et al., 1990; Haynes and Barton, 1990; Álvarez-Salgado et al., 2003; Torres and Barton, 2006). Thus, the IPC that typically occurs during autumn and winter (Frouin et al., 1990; Haynes and Barton, 1990; Peliz et al., 2005) when meridional density gradients are the strongest and southerly winds dominate in the region (Wooster et al., 1976; Figueiras et al., 2002; Álvarez-Salgado et al., 2003), can also be observed in spring during periods of strong southerly winds (Mazé et al., 1997; Fiúza et al., 1998; Álvarez-Salgado et al., 2003).

In May 1993, intense southwesterly winds (Fig. 1b), although preceded by upwelling favourable northerly winds, promoted the formation of the IPC which was well defined by salty waters (S > 35.9, Fig. 2b). The observed weak thermal signal of this spring IPC (Fig. 2a) was due to the previous cooling and strong mixing that regularly take place in winter and that leaves the IPC with an upper mixed layer of ~150m and temperatures of ~14 ºC (Álvarez-Salgado et al., 2003). In early spring, the incipient solar heating was sufficient to develop weakly stratified conditions (Figs. 3a-e) but not strong enough to allow the differentiation between IPC and coastal waters. The clearest thermal signature of the IPC, with surface temperatures of ~20 ºC, occurs in autumn (Álvarez-Salgado et al., 2003), when stratification is stronger and cool upwelled waters still remain on the shelf.

293 Corresponding geopotential anomaly computations (Figueiras et al, 1998; Álvarez-
294 Salgado et al., 2003) indicated the existence of opposed flows north and south of 42ºN
295 (Fig. 2b), where the main entry of oceanic waters to form the IPC occurred (Fig. 3h).
296 While the IPC demonstrated poleward flow in the north, flow in the south was
297 predominantly equatorward, indicating that the oceanic intrusion diverged once it
298 reached the continental slope. There was also a weak southward flow in the northwest
299 corner, outside of the IPC, where salinity was < 35.9 (Fig. 2b). This flow, which appears
300 to be a permanent feature of the circulation in the Iberian Basin even when the IPC is
301 present (Ambar and Fiúza, 1994; Peliz et al., 2005), transports colder and fresher water
302 from the north and confines the IPC to the slope in the northern area (Peliz et al., 2005).
303 This confinement of the IPC promotes the development of downwelling at the shelf
304 break. The existence of convergent and divergent fronts associated with the IPC is a
305 well known feature (Fernández et al., 1991; Castro et al., 1997; Álvarez-Salgado et al.,
306 2003). The convergent front near the shelf break prevents the oceanward extension of
307 shelf waters, whereas the more diffuse divergence front on the ocean side separates the
308 subtropical waters of the IPC from the less saline oceanic waters transported from the
309 north (Fig. 2b).
310 Although winter mixing injects nitrate (1.5-2.0 μmol kg^{-1}) into the surface layer
311 (Álvarez-Salgado et al., 2003), the low nitrate and chl *a* concentrations recorded in the
312 surface waters of the IPC in May 1993 suggest that the spring bloom had already
313 occurred. This view is also supported by the existence of a nutricline and its associated
314 chl *a* maximum, as well as by the dominance of a microplankton assemblage (negative
315 values of PC2) in which heterotrophic ciliates (Strombidium turbo, Strombidium
316 strobilum and Strombidium conicum) were important components (Figs. 7a, 8a-c). The
317 presence of ciliates tends to suggest the existence of regenerative processes.

318 The dominance of small flagellates, the absence of diatoms and a low contribution
319 of small dinoflagellates constituted an assemblage that has been reported previously for
320 other IPCs in autumm (Castro et al., 1997) and spring (Bode et al., 1990; Fernández et
321 al., 1991). In general, the IPC is characterised by the almost exclusive dominance of
322 pico-nanoplankton communities with a minor contribution of microplankton (Tilstone et
323 al., 2003; Calvo-Díaz et al., 2004; Lorenzo et al., 2005). This dominance of small
324 phytoplankton forms, but specifically the absence of diatoms, corroborates the oceanic
325 origin of the poleward waters (Malone et al., 1983).
326 The microplankton distributions (Figs. 5, 6) also serve to confirm that the primary
327 effect of the IPC is to prevent across-shelf exchange and, therefore, the oceanic export
328 of coastal microplankton (Castro et al., 1997; Álvarez-Salgado et al., 2003). The
329 distributions of diatoms were especially informative to this respect (Figs. 5b, 6c-e), as
330 they were confined to the coast. The distributions of diatoms and dinoflagellates in the
331 north (Figs. 5bc, 6af) also demonstrate that the IPC, while progressing to the north,
332 broke the across-shelf microplankton distribution typical of the previous upwelling
333 event, characterised by the dominance of diatoms in coastal waters and a higher
334 importance of dinoflagellates towards the open ocean (Tilstone et al., 1994). Episodes
335 of similar intrusions, leaving different microplankton populations on and off the shelf,
336 have also been described for northern Iberia in spring (Bode et al., 1990; Fernández et
337 al., 1991).
338 The distributions of the PC2 and PC3 scores (Figs. 7, 8) showed a spatial
339 segregation of microplankton assemblages on the shelf that must be related to different
340 stages of succession (Margalef, 1958). The microplankton assemblage in the SE, with
341 dominance of large heterotrophic and autotrophic dinoflagellates (Gyrodinium spirale
342 and Gymnodnium catenatum, positive loads with PC2), is typical of a later stage of the

succession than the diatom assemblage (positive loads with PC3) dominating further north (Figueiras and Niell, 1987; Figueiras and Ríos, 1993). The more advanced stage of the succession in the south is also confirmed by the presence of the toxic dinoflagellate G. catenatum, which usually appears in the north, in front of the Rías Baixas, during summer and autumn (e.g. Fraga et al., 1988; Figueiras et al., 1994; Fermín et al., 1996). The higher negative scores of PC3 (Lingulodinium polyedrum and Ceratium furca) in the south than in the north (Figs. 7b, 8f-j) also support this view, since both dinoflagellates are recurrent components of the summer-autumn assemblages in the north (Figueiras and Ríos, 1993; Castro et al., 1997).

Despite the reduced importance of diatoms on the southern shelf, the location of the diatom assemblage (positive values of PC3) at a deeper level than the large dinoflagellate assemblage (positive values of PC2) (Figs. 8d,e,i,j) indicates that the IPC intrusion caused a vertical segregation of microplankton. This might be forced by the onshore flow and near-shore sinking associated with the IPC, which could transpose the horizontal surface distribution of microplankton associated with the previous upwelling to the vertical dimension near the coast. Surface microplankton distribution during upwelling is characterised by diatom dominance in coastal waters (positive values of PC3) and a higher importance of large dinoflagellates at the oceanic side (positive values of PC2) (Margalef, 1978; Tilstone et al., 1994). After this transposition and under suitable downwelling conditions, the vertical swimming capability of large dinoflagellates (Eppley and Harrison, 1975; Cullen, 1985; Fraga et al., 1992), in opposition to the passive behaviour of diatoms, would allow them to counteract the downward velocities and, hence, to remain in the surface layers for the initiation of a bloom (Fraga et al., 1988; Figueiras et al, 1994; Fermín et al., 1996).] Thus, it appears that the IPC, through the action of downwelling, selects for the local microplankton

populations instead of transporting them to the north. This view is also supported by the distribution of Gymnodinium catenatum, which does not point to its northward transport.

5. Conclusion

The spring IPC instead of transporting HABs creates the suitable environmental conditions to trigger them. This action occurs through the downwelling and the associated onshore-downward currents generated by the IPC on the shelf, which remove diatoms from the water column and allow the selection of dinoflagellates. Although more research is needed to corroborate this single observation, we suggest that the northward spreading of HABs on the west coast of Iberia is related to the interaction of the IPC and the latitudinal progression of microplankton succession on the shelf, rather than the northward transport of harmful species by the IPC. This explanation is consistent with the more frequent occurrence of HABs in the north, specifically in the Rias Baixas region, during late summer-early autumn, since this is the time when the local microplankton community is likely to contain potentially harmful dinoflagellates and corresponds to the onset of the IPC.

Acknowledgements

We wish to thank the captain and crew of the RV ‘Cornide de Saavedra’ and the participants in the MORENA I cruise for their help. Special thanks to C.G. Castro for useful suggestions. Financial support for this work came from the EU MORENA project (MAS-CT93-0065) and the EU HABILE project (EVK3-CT-2001-00063). B.G.C. was funded by a predoctoral I3P fellowship of CSIC-European Social

Foundation. This is a contribution to the GEOHAB Core Research Project – HABs in Upwelling Systems.

References

Álvarez-Salgado, X.A., Figueiras, F.G., Pérez, F.F., Groom, S., Nogueira, E., Borges, A.V., Chou, L., Castro, C.G., Moncoiffé, G., Ríos, A.F., Miller, A.E.J., Frankignoulle, M., Savidge, G., Wollast, R., 2003. The Portugal coastal counter current off NW Spain: new insights on its biogeochemical variability. Progr. Oceanogr. 56, 281-321.

Ambar, I., Fiúza, A.F.G., 1994. Some features of the Portugal current system: a poleward slope undercurrent, an upwelling-related summer southward flow and an autumn-winter poleward surface current. In: Katsaros, K.B., Fiúza, A.F.G., Ambar, I. (Eds.), Proceedings of the second international conference on air-sea interaction and on meteorology and oceanography of the coastal zone. American Meteorological Society, Boston, pp. 286-287.

Anderson, D.M., Gilbert, P.M., Burkholder, J.M., 2002. Harmful algal blooms and eutrophication: Nutrient sources, composition and consequences. Estuaries 25, 704-726.

Anderson, D.M., Keafer, B.A., Geyer, W.R., Signell, R.P., Loder, T.C., 2005. Toxic Alexandrium blooms in the western Gulf of Maine: The plume advection hypothesis revisited. Limnol. Oceanogr. 50, 328-345.

Bode, A., Fernández, E., Botas, A., Anadón, R. 1990., Distribution and composition of suspended particular matter related to shelf-break salinity intrusion in the Cantabrian Sea (Bay of Biscay). Oceanol. Acta 13, 219-228.

416 Calvo-Díaz, A., Morán, X.A.G., Nogueira, E., Bode, A., Varela, M., 2004. Picoplankton
417 community structure along the northern Iberian continental margin in late winter-
418 early spring. J. Plankton Res. 26, 1069-1081.
419 Castro, C.G., Álvarez-Salgado, X.A., Figueiras, F.G., Pérez, F.F., Fraga, F., 1997.
420 Transient hydrographic and chemical conditions affecting microplankton populations
421 in the coastal transition zone of the Iberian upwelling system (NW Spain) in
422 September 1986. J. Mar. Res. 55, 321-352.
423 Cullen, J.J., 1985. Diel vertical migration by dinoflagellates: roles of carbohydrate
424 metabolism and behavioural flexibility. In: Rankin, M.A. (Ed.), Migration:
425 mechanisms and adaptative significance. Univ. Texas Mar. Sci. Inst. Suppl. 27, 135-
426 152.
427 Eppley, R.W., Harrison, W.O., 1975. Physiological ecology of Gonyaulax polyedra, a
428 red water dinoflagellate of Southern California. In: LoCicero, V. (Ed.), Toxic
429 Dinoflagellate Blooms. Massachusetts Science Technological Foundation,
430 Wakefield, pp. 11-22.
431 Estrada, M., 1995. Dinoflagellate assemblages in the Iberian upwelling area. In: Lassus,
432 P., Arzul, G., Erard, E., Gentien, P., Marcaillou, C. (Eds.), Harmful Marine Algal
433 Blooms. Technique et Documentation-Lavoisier, Intercept Ltd, Paris, pp. 157-162.
434 Fermín, E.G., Figueiras, F.G., Arbones, B., Villarino, M.L., 1996. Short-time scale
435 development of a Gymnodinium catenatum population in the Ría de Vigo (NW
436 Spain). J. Phycol. 32, 212-221.
437 Fernández, E., Bode, A., Botas, A., Anadón, R., 1991. Microplankton assemblages
438 associated with saline fronts during a spring bloom in the central Cantabrian Sea:
439 differences in trophic structure between water bodies. J. Plankton Res. 13, 1239-
440 1256.

441 Figueiras, F.G., Álvarez-Salgado, X.A., Castro, C.G., Villarino, M.L., 1998.
442 Accumulation of Gymnodinium catenatum Graham cells in western Iberian shelf
443 waters in response to poleward flowing slope currents. In: Reguera, B., Blanco, J.,
444 Fernández, M.L., Wyatt, T. (Eds.), Harmful algae. Xunta de Galicia and
445 intergovernmental oceanographic commission of UNESCO 1998, Paris, pp. 114-117.
446 Figueiras, F.G., Jones, K.J., Mosquera, A.M., Álvarez-Salgado, X.A., Edwards, A.,
447 MacDougall, N., 1994. Red tide assemblage formation in an estuarine upwelling
448 ecosystem: Ria de Vigo. J. Plankton Res. 16, 857-878.
449 Figueiras, F.G., Labarta, U., Fernández Reiriz, M.J., 2002. Coastal upwelling, primary
450 production and mussel growth in the Rías Baixas of Galicia. Hydrobiologia 484,
451 121-131.
452 Figueiras, F.G., Niell, F.X., 1987. Composición del fitoplancton en la ría de Pontevedra,
453 NO de España. Inv. Pesq. 51, 371-409.
454 Figueiras, F.G., Pazos, Y., 1991. Hydrography and phytoplankton of the Ria de Vigo
455 before and during a red tide of Gymnodinium catenatum Graham. J. Plankton Res.
456 13, 589-608.
457 Figueiras, F.G., Ríos, A.F., 1993. Phytoplankton succession, red tides and the
458 hydrographic regime in the Rías Bajas of Galicia. In: Smayda, T.J., Shimizu, Y.
459 (Eds.), Toxic phytoplankton blooms in the Sea. Elsevier, New York, pp. 239-244.
460 Fiúza, A.F.G., Hamann, M., Ambar, I., Díaz del Río, G., González, N., Cabanas, J.M.,
461 1998. Water masses and their circulation off western Iberia during May 1993. Deep-
462 Sea Res. I 45, 1127-1160.
463 Fraga, F., Pérez, F.F., Figueiras, F.G., Ríos, A.F., 1992. Stoichiometric variations of N,
464 P, C and O_2 during a Gymnodinium catenatum red tide and their interpretation. Mar.
465 Ecol. Prog. Ser. 87, 123-134.

466 Fraga, S., Anderson, D.M., Bravo, I., Reguera, B., Steidinger, K.A., Yentsch, C.M.,
467 1988. Influence of upwelling relaxation on dinoflagellates and shellfish toxicity in
468 Ria de Vigo, Spain. Est. Coast. Shelf Sci. 27, 349-361.
469 Fraga, S., Bravo, I., Reguera, B., 1993. Poleward surface current at the shelf break and
470 blooms of Gymnodinium catenatum in Ria de Vigo (NW Spain). In: Smayda, T.J.,
471 Shimizu, Y. (Eds.), Toxic phytoplankton blooms in the sea. Elsevier, New York, pp.
472 245-249.
473 Franks, P.J.S., Anderson, D.M., 1992. Alongshore transport of a toxic phytoplankton
474 bloom in a buoyancy current: Alexandrium tamarense in the Gulf of Maine. Mar.
475 Biol. 112, 153-164.
476 Frouin, R., Fiúza, A.F.G., Ambar, I., Boyd, T.J., 1990. Observations of a poleward
477 surface current off the coasts of Portugal and Spain during winter. J. Geophys. Res.
478 95, 679-691.
479 GEOHAB, 2001. Global Ecology and Oceanography of Harmful Algal Blooms, Science
480 Plan. In: Glibert, P., Pitcher, G.C. (Eds.), SCOR and IOC, Baltimore and Paris
481 Hansen, H., Grasshoff, K., 1983. Automated chemical analysis. In: Grasshoff, K.,
482 Ehrardt, M., Kremling, K. (Eds.), Methods of seawater analysis, Verlag Chemie,
483 Weinheim, pp. 347-395.
484 Haynes, R., Barton, E.D., 1990. A poleward flow along the Atlantic coast of the Iberian
485 Peninsula. J. Geophys. Res. 95, 11425-11441.
486 Hidy, G.M., 1972. A review of recent air-sea interaction research. Bull. Am. Meteorol.
487 Soc. 53, 1083-1102.
488 Lorenzo, L.M., Arbones, B., Tilstone, G.H., Figueiras, F.G., 2005. Across-shelf
489 variability of phytoplankton composition, photosynthetic parameters and primary
490 production in the NW Iberian upwelling system. J. Mar. Syst. 54, 157-173.

491 Malone, T.C., Hopkins, T.S., Falkowski, P.G., Whitledge, T.E., 1983. Production and
492 transport of phytoplankton biomass over the continental shelf of the New York
493 Bight. Cont. Shelf Res. 1, 305-337.
494 Margalef, R., 1956. Estructura y dinámica de la “purga de mar” en la Ría de Vigo. Inv.
495 Pesq. 5, 113-134.
496 Margalef, R., 1958. Temporal succession and spatial heterogeneity in phytoplankton. In:
497 Buzzati-Traverso, A.A. (Ed.), Perspectives in marine biology. University California
498 Press, Berkeley, pp. 323-349.
499 Margalef, R., 1978. Phytoplankton communities in upwelling areas. The example of
500 NW Africa. Oecologia Aquatica 3, 97-132.
501 Mazé, J.P., Arhan, M., Mercier, H., 1997. Volume budget of the eastern boundary layer
502 off the Iberian Peninsula. Deep-Sea Res. I 44, 1543-1574.
503 Moita, M.T., Vilarinho, M.G., Palma, A.S., 1998. On the variability of Gymnodinium
504 catenatum Graham blooms in Portuguese waters. In: Reguera, B., Blanco, J.,
505 Fernández, M.L., Wyatt, T. (Eds.), Harmful Algae. Xunta de Galicia and
506 Intergovernmental Oceanographic Commission of UNESCO, Paris, pp. 118-121.
507 Mouriño, C., Fraga, F., 1985. Determinación de nitratos en agua de mar. Inv. Pesq. 49,
508 81-96.
509 Peliz, A., Dubert, J., Santos, A.M.P., Oliveira, P.B., Le Cann, B., 2005. Winter upper
510 ocean circulation in the Western Iberian Basin-fronts, eddies and poleward flows: an
511 overview. Deep-Sea Res. I 52, 621-646.
512 Pingree, R.D., Le Cann, B., 1990. Structure, strength and seasonality of the slope
513 currents in the Bay of Biscay region. J. Mar. Biol. Assoc. UK 70, 857-885.
514 Pingree, R.D., Sinha, B., Griffiths, C.R., 1999. Seasonality of the European slope
515 current (Goban Spur) and ocean margin exchange. Cont. Shelf Res. 19, 929-975.

516 Pitcher, G.C., Boyd, A.J., 1996. Cross-shelf and along-shore dinoflagellate distributions
517 and the mechanism of red tide formation within the southern Benguela upwelling
518 system. In: Yasumoto, T., Oshima, Y., Fukuyo, Y. (Eds.), Harmful and Toxic Algal
519 Blooms. IOC of UNESCO, Paris, pp. 243-246.
520 Pitcher, G.C., Boyd, A.J., Horstman, D.A., Mitchell-Innes, B.A., 1998. Subsurface
521 dinoflagellate populations, frontal blooms and the formation of red tide in the
522 southern Benguela upwelling system. Mar. Ecol. Prog. Ser. 172, 253-264.
523 Raine, R., McMahon, T., 1998. Physical dynamics on the continental shelf off
524 southwestern Ireland and their influence on coastal phytoplankton blooms. Cont.
525 Shelf Res. 18, 883-914.
526 Ryan, J.P., Dierssen, H.M., Kudela, R.M., Scholin, C.A., Johnson, K.S., Sullivan, J.M.,
527 Fischer, A.M., Rienecker, E.V., Mcenaney, P.R., Chavez, F.P., 2005. Coastal ocean
528 physics and red tides: an example from Monterey Bay, California. Oceanography 18,
529 246-255.
530 Smayda, T.J., 1990. Novel and nuisance phytoplankton blooms in the sea: evidence for
531 a global epidemic. In: Granéli, E., Sundström, B., Edler, L., Anderson, D.M. (Eds.),
532 Toxic marine phytoplankton. Elsevier, New York, pp. 29-40.
533 Sordo, I., Barton, E.D., Cotos, J.M., Pazos, Y., 2001. An inshore poleward current in the
534 NW of the Iberian Peninsula detected from satellite images, and its relation with G.
535 catenatum and D. acuminata blooms in the Galician rias. Est. Coast. Shelf Sci. 53,
536 787-799.
537 Tester, P.A., Steindinger, K.A., 1997. Gymnodnium breve red tide blooms: Initiation,
538 transport, and consequences of surface circulation. Limnol. Oceanogr. 42, 1039-
539 1051.

Tester, P.A., Stumpf, R.P., Vukovich, F.M., Fowler, P.K., Turner, J.T., 1991. An expatriate red tide bloom: Transport, distribution, and persistence. Limnol. Oceanogr. 36, 1053-1061.

Tilstone, G.H., Figueiras, F.G., Fraga, F., 1994. Upwelling-downwelling sequences in the generation of red tides in a coastal upwelling system. Mar. Ecol. Prog. Ser. 112, 241-253.

Tilstone, G.H., Figueiras, F.G., Lorenzo, L.M., Arbones, B., 2003. Phytoplankton composition, photosynthesis and primary production during different hydrographic conditions at the NW Iberian upwelling system. Mar. Ecol. Progr. Ser. 252, 89-104.

Torres, R., Barton, E.D., 2006. Onset and development of the Iberian poleward flow along the Galician coast. Cont. Shelf Res. 26, 1134-1153.

Trainer, V.L., Hickey, B.M., Horner, R.A., 2002. Biological and physical dynamics of domoic acid production off the Washington coast. Limnol. Oceanogr. 47, 1438-1446.

Wooster, W.S., Bakun, A., McLain, D.R., 1976. The seasonal upwelling cycle along the eastern boundary of the North Atlantic. J. Mar. Res. 34, 131-141.

555 Table 1. Correlation coefficients (loads) of the species and taxa selected for Principal
556 Component Analysis (PCA) with the first 3 principal components. Species and taxa are
557 ordered according to PC1. The highest positive and negative loads for PC2 and PC3 are
558 in bold. The groups are (Diat) diatoms, (Dinof) dinoflagellates, (Flag) flagellates other
559 than dinoflagellates and (Cil) ciliates

Group	Taxon	PC1	PC2	PC3
Dinof	Heterocapsa niei	0.722	-0.117	-0.002
Cil	Strombidium cornutum	0.665	-0.144	-0.160
Cil	Strombidium ovale	0.624	-0.168	-0.100
Cil	Strombidium sulcatum	0.605	-0.231	-0.011
Dinof	Ceratium fusus	0.578	0.311	-0.214
Diat	Proboscia alata	0.562	**0.493**	-0.174
Dinof	Protoperidinium divergens	0.560	0.134	-0.272
Diat	Pseudo-nitzschia cf. seriata	0.547	0.283	**0.420**
Dinof	Prorocentrum minimum	0.532	-0.076	0.129
Dinof	Gymnodinium catenatum	0.518	**0.467**	-0.250
Flag	Unidentified small flagellates	0.517	**-0.508**	0.208
Dinof	Ceratium horridum	0.512	0.396	-0.230
Dinof	Amphidoma caudata	0.501	0.065	-0.131
Dinof	Ceratium furca	0.496	-0.295	**-0.403**
Dinof	Amphidinium flagellans	0.488	-0.272	0.175
Dinof	Lingulodinium polyedrum	0.462	-0.282	**-0.475**
Flag	Solenicola setigera	0.442	**0.427**	0.151
Diat	Leptocylindrus danicus	0.423	0.219	**0.482**
Dinof	Torodinium robustum	0.419	-0.147	0.031
Dinof	Small Gymnodinium spp.	0.416	**-0.406**	0.181
Dinof	Mesoporos perforatus	0.415	0.209	-0.372
Dinof	Cochlodinium helix	0.404	0.338	0.220
Dinof	Gymnodinium nanum	0.400	**-0.494**	0.159
Diat	Guinardia flaccida	0.368	0.374	0.381
Flag	Criptophyceae spp.	0.367	**-0.644**	0.072
Flag	Dictyocha fibula	0.364	0.343	-0.034
Dinof	Gyrodinium fusiforme	0.333	0.060	-0.151
Diat	Small centric diatoms	0.317	0.109	**0.445**
Cil	Mesodinium rubrum	0.316	0.194	**0.433**
Dinof	Small Dinophysis spp.	0.302	0.119	0.253
Dinof	Gymnodinium varians	0.294	-0.265	0.024
Cil	Strombidium turbo	0.282	**-0.521**	0.178
Dinof	Cysts of dinoflagellates	0.268	0.075	-0.186
Dinof	Gyrodinium spirale	0.260	**0.519**	-0.055

Dinof	Protoperidinium pyriforme	0.229	-0.092	-0.235
Cil	Strombidium conicum	0.206	**-0.401**	0.107
Cil	Strombidium strobilum	0.196	**-0.512**	-0.072
Cil	Strobilidium spiralis	0.097	0.039	**0.471**
Diat	Guinardia delicatula	0.003	0.156	0.393
Dinof	Gymnodinium agiliforme	0.001	**-0.449**	0.150
Dinof	Cystodinium steinii	-0.092	0.104	0.196

560
561

562 **Figure captions**

563

564 Fig. 1. (a) Map of the sampling region in the western Iberian margin; the sections
565 selected for vertical representations in figures 3, 4, 6 8 and 9 are indicated. (b) Ekman
566 transport components, -Qx (cross-shore transport) and Qy (along-shore transport),
567 during May 1993 calculated at 43ºN 11ºW. Dashed area denotes the sampling period.

568

569 Fig. 2. Surface distributions of (a) temperature, (b) salinity, (c) nitrate concentration and
570 (d) chlorophyll concentration in the sampled region off western Iberian Peninsula.
571 Dashed line in (c) and (d) corresponds to the isohaline of 35.9 in (b) and represents the
572 Iberian Poleward Current (IPC) domain. Black arrows in (b) represent the main
573 geostrophic flow pattern in the sampled region. More details are given in the discussion.

574

575 Fig. 3. Vertical distributions at the five selected sections (see Fig. 1a) of (a-e)
576 temperature and (f-j) salinity with shaded areas indicating the IPC domain.

577

578 Fig. 4. Vertical distributions at the five selected sections (see Fig. 1a) of (a-e) nitrate and
579 (f-j) chlorophyll concentrations.

580

581 Fig. 5. Surface distributions of abundance of (a) total microplankton, (b) diatoms, (c)
582 dinoflagellates and (d) flagellates other than dinoflagellates. Dashed line represents the
583 IPC domain defined by the 35.9 isohaline (see Fig. 2b).

584

585 Fig.6. Vertical distributions at the five selected sections (see Fig. 1a) of abundance of
586 (a-e) diatoms, (f-j) dinoflagellates and (k-o) flagellates other than dinoflagellates.

Fig. 7. Surface distributions of (a) PC 2 and (b) PC 3 scores extracted by the principal component analysis of microplankton species abundance. Dashed line represents the IPC domain defined by the 35.9 isohaline (see Fig. 2b).

Fig. 8. Vertical distributions at the five selected sections (see Fig. 1a) of (a-e) PC 2 and (f-j) PC 3 scores extracted by principal components analysis of microplankton species abundance.

Fig. 9. Distributions of the abundance of Gymnodinium catenatum at (a) the sea surface and (b, c) the southernmost sections where it was present. Dashed line in (a) represents the IPC domain defined by the 35.9 isohaline (see Fig. 2b).

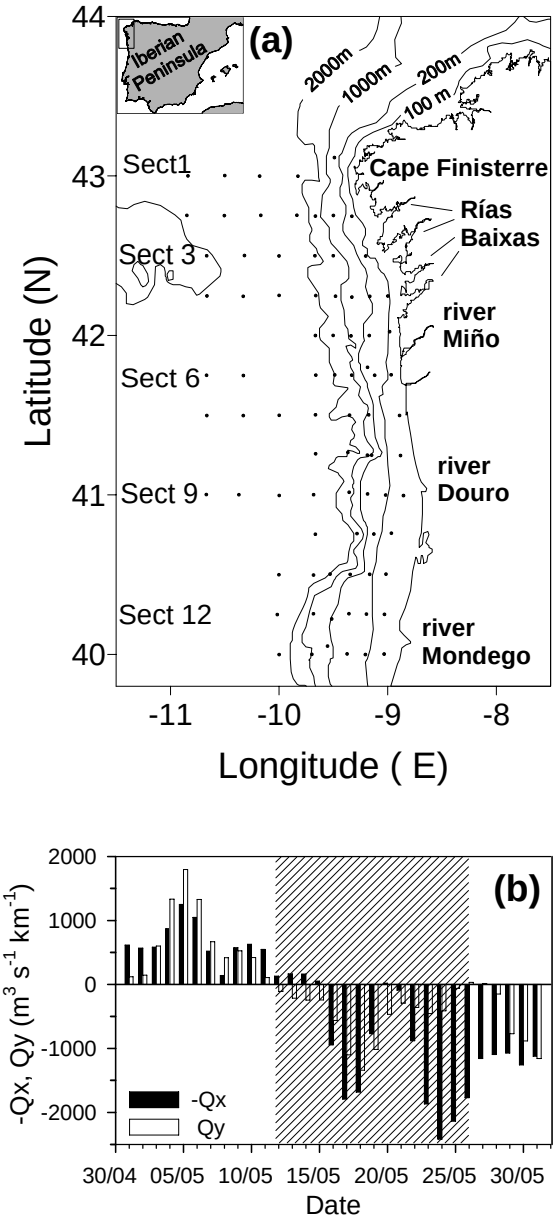

Fig. 1
Crespo & Figueiras

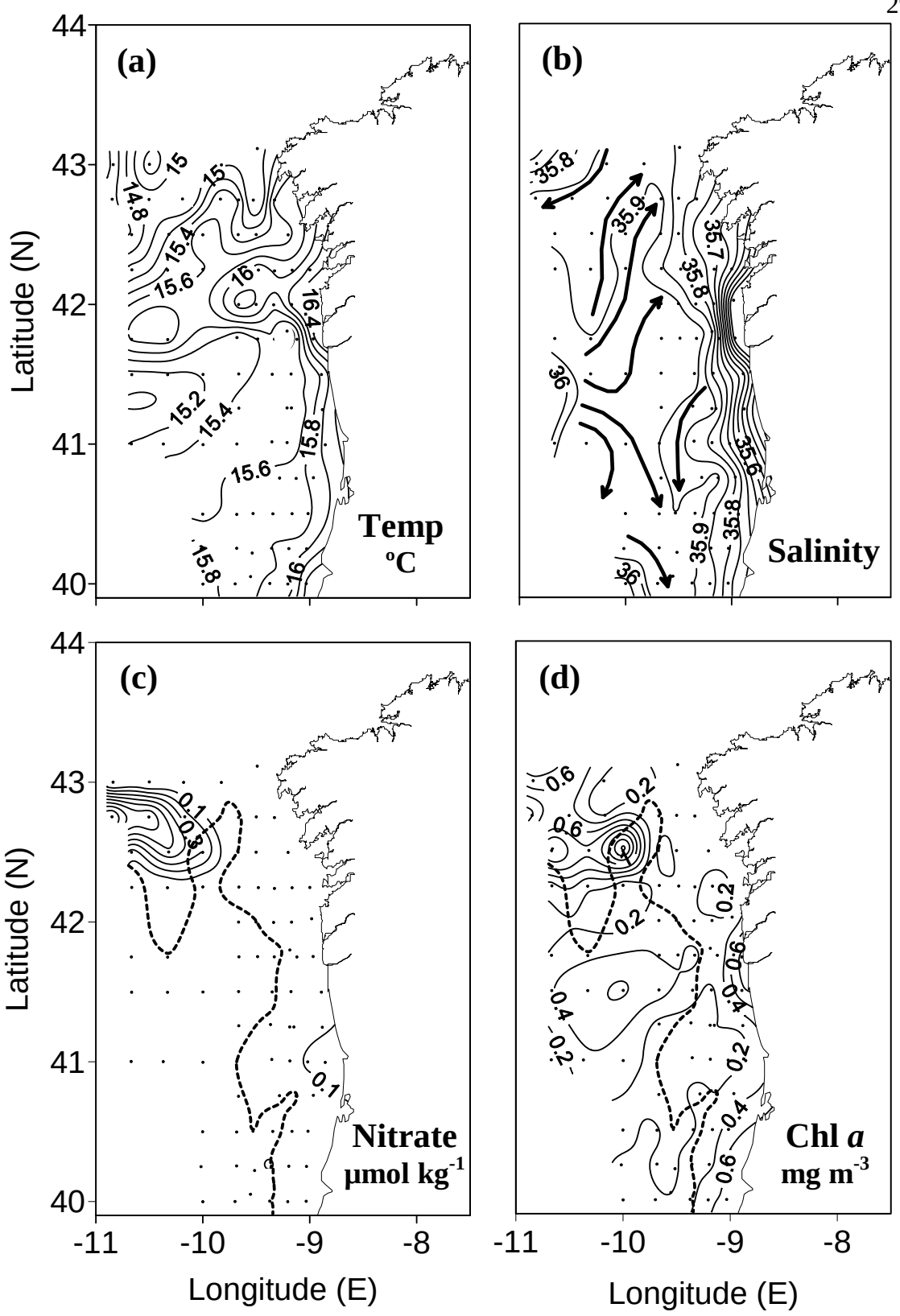

Fig. 2
Crespo & Figueiras

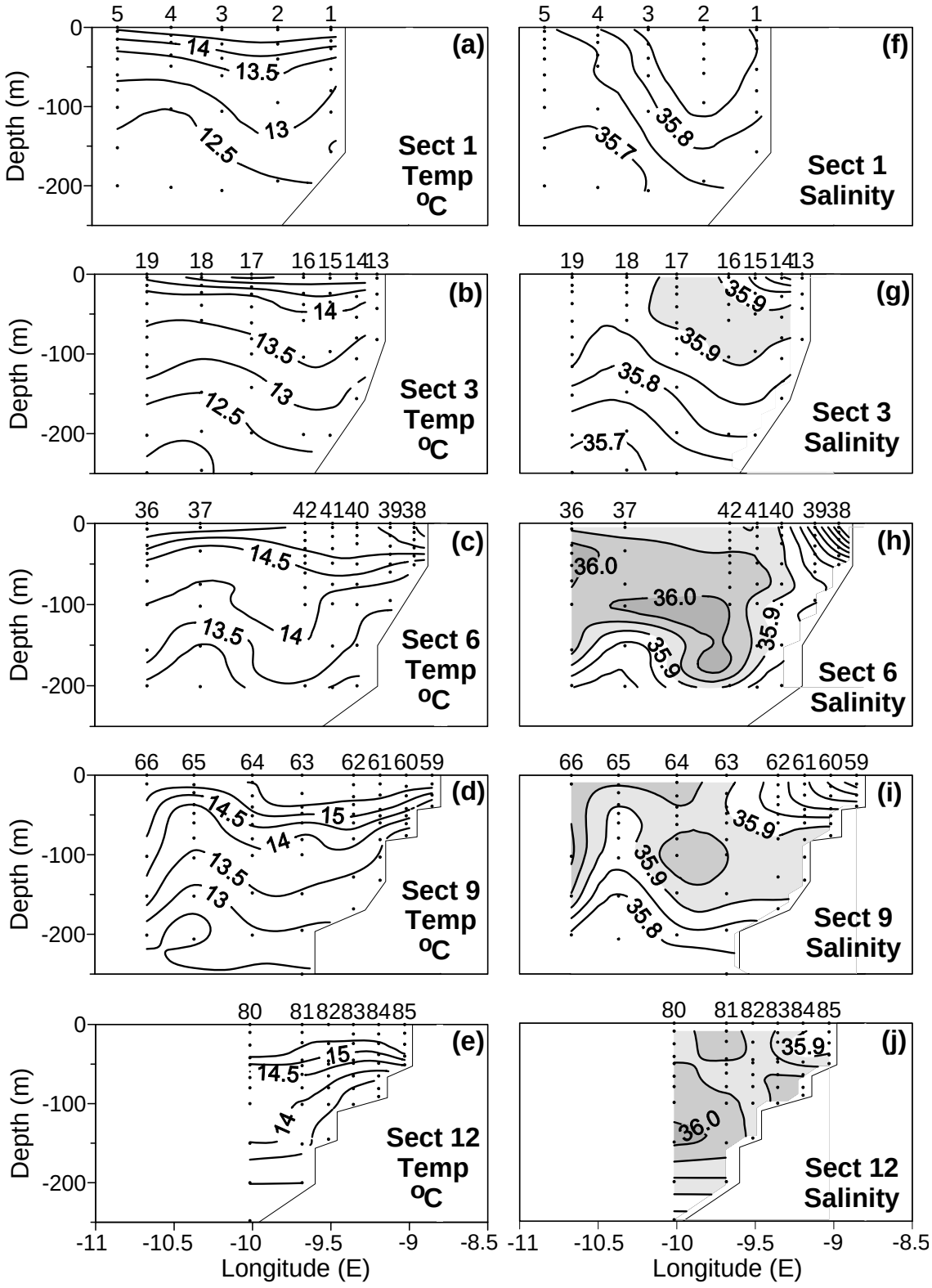

Fig. 3
Crespo & Figueiras

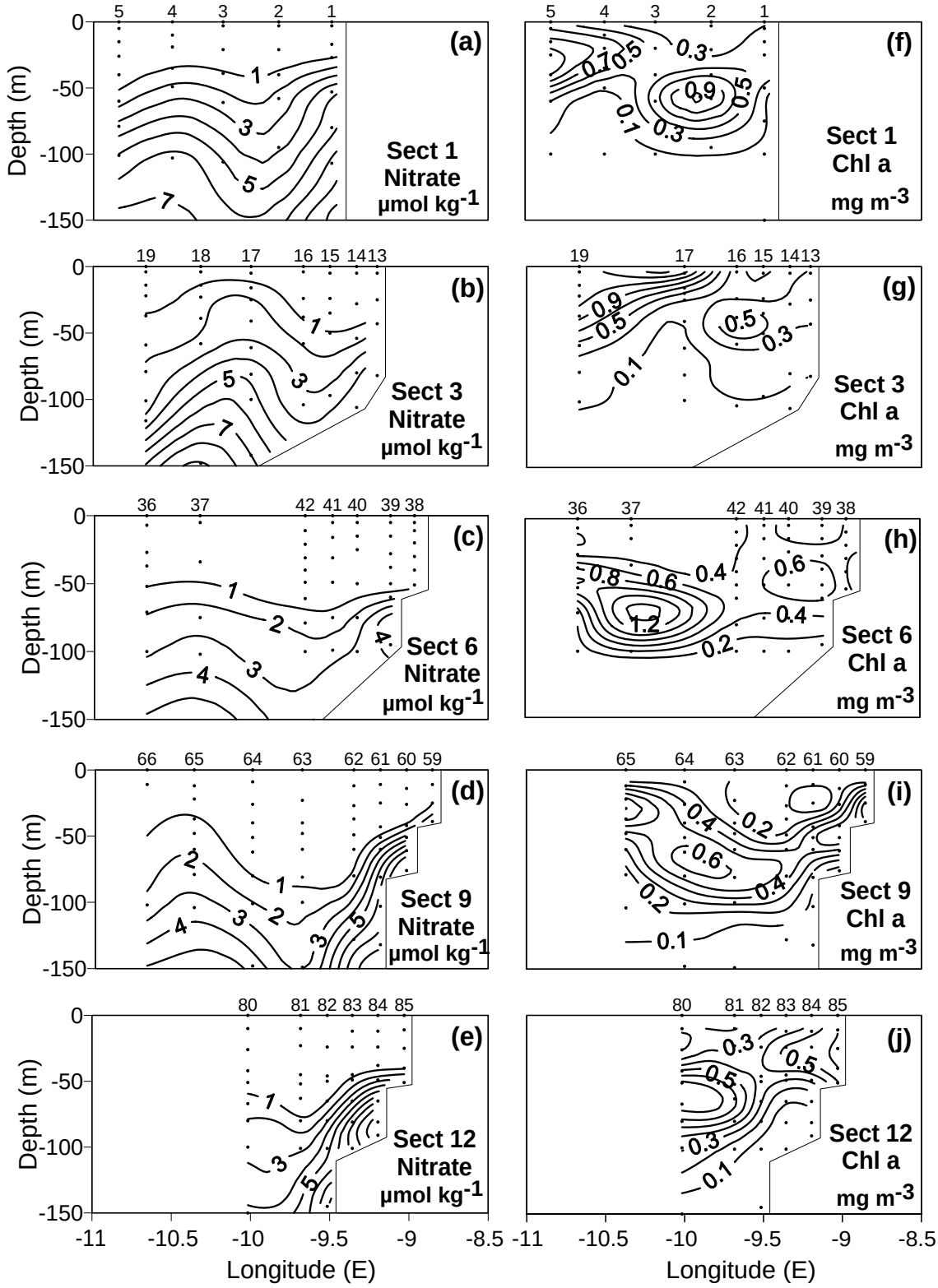

Fig. 4
Crespo & Figueiras

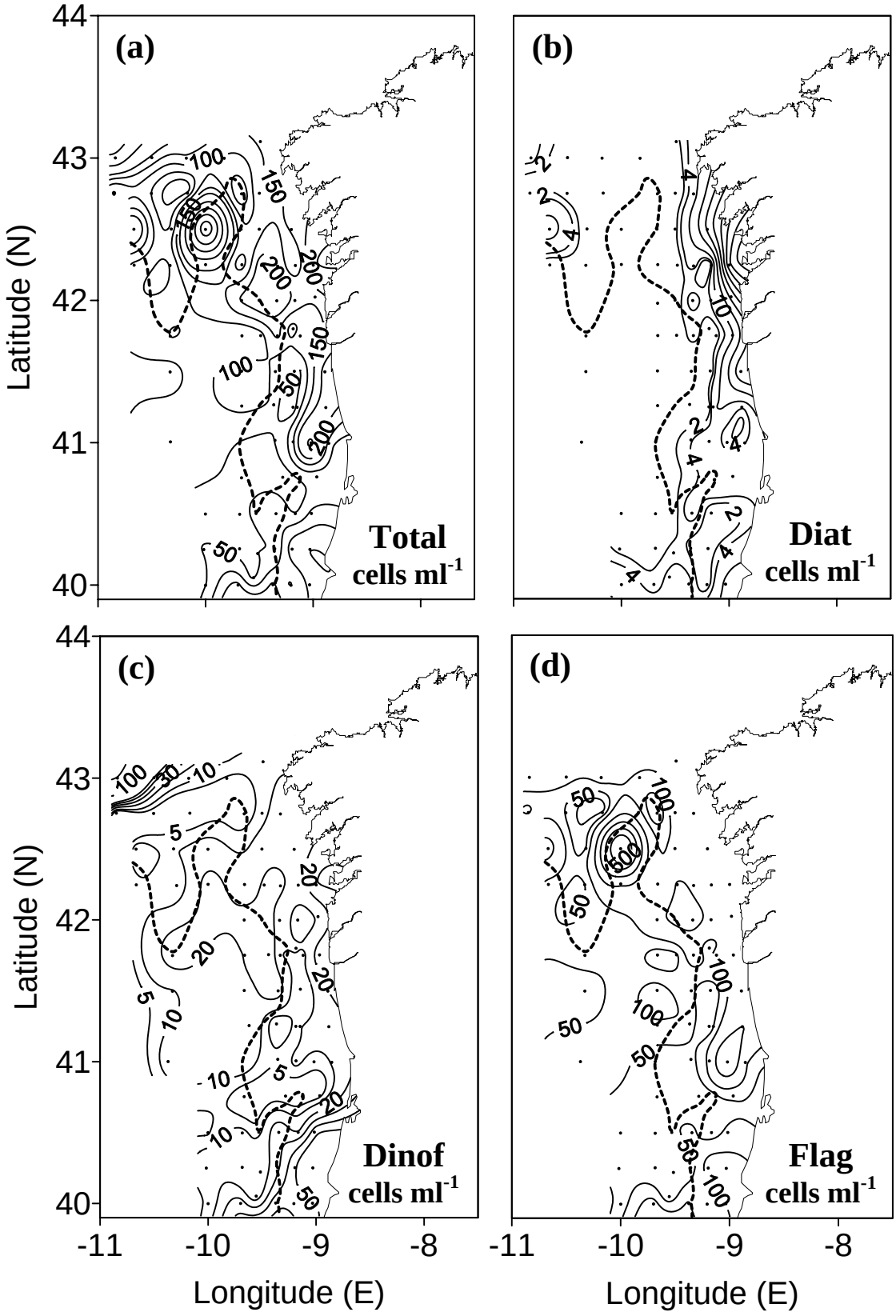

Fig. 5
Crespo & Figueiras

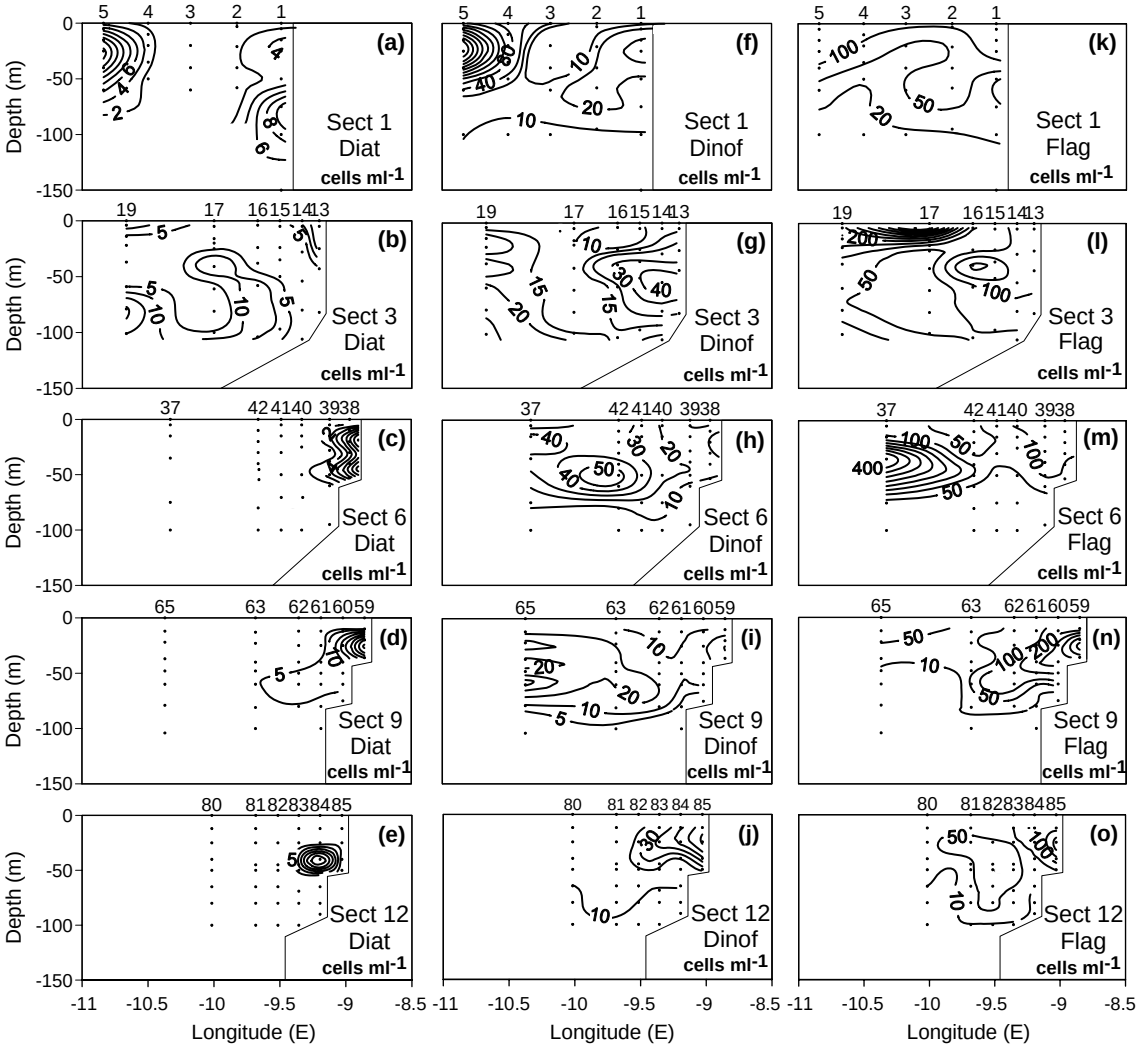

Fig. 6
Crespo & Figueiras

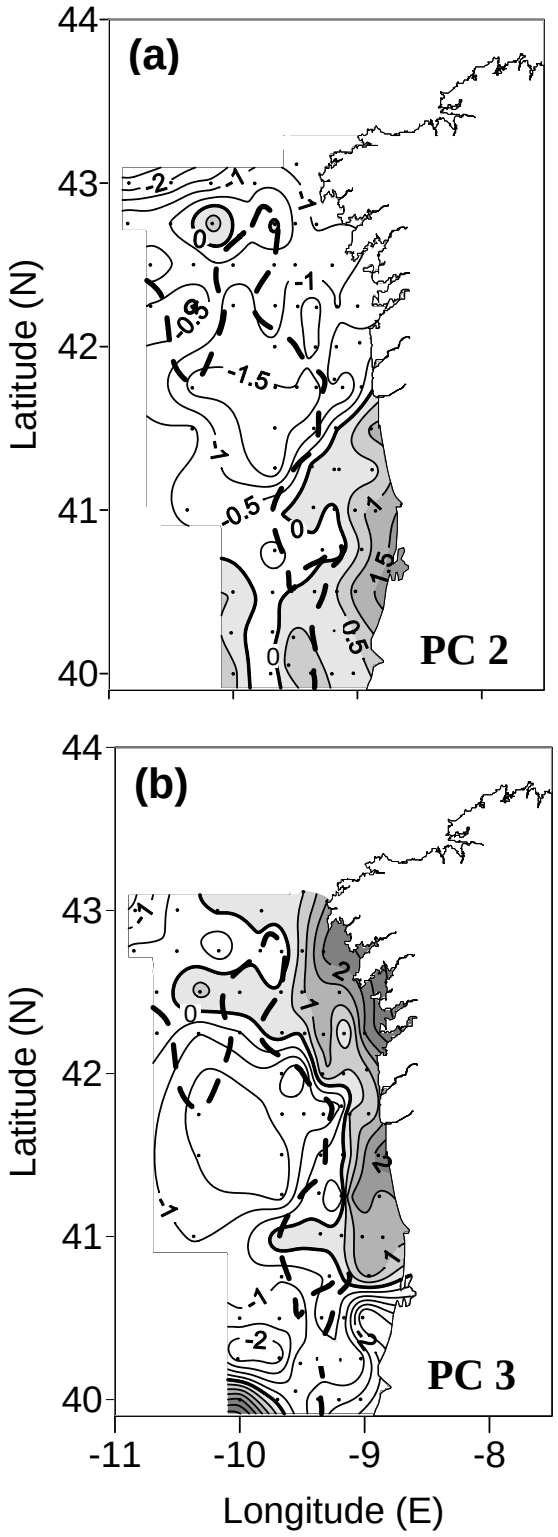

Fig. 7
Crespo & Figueiras

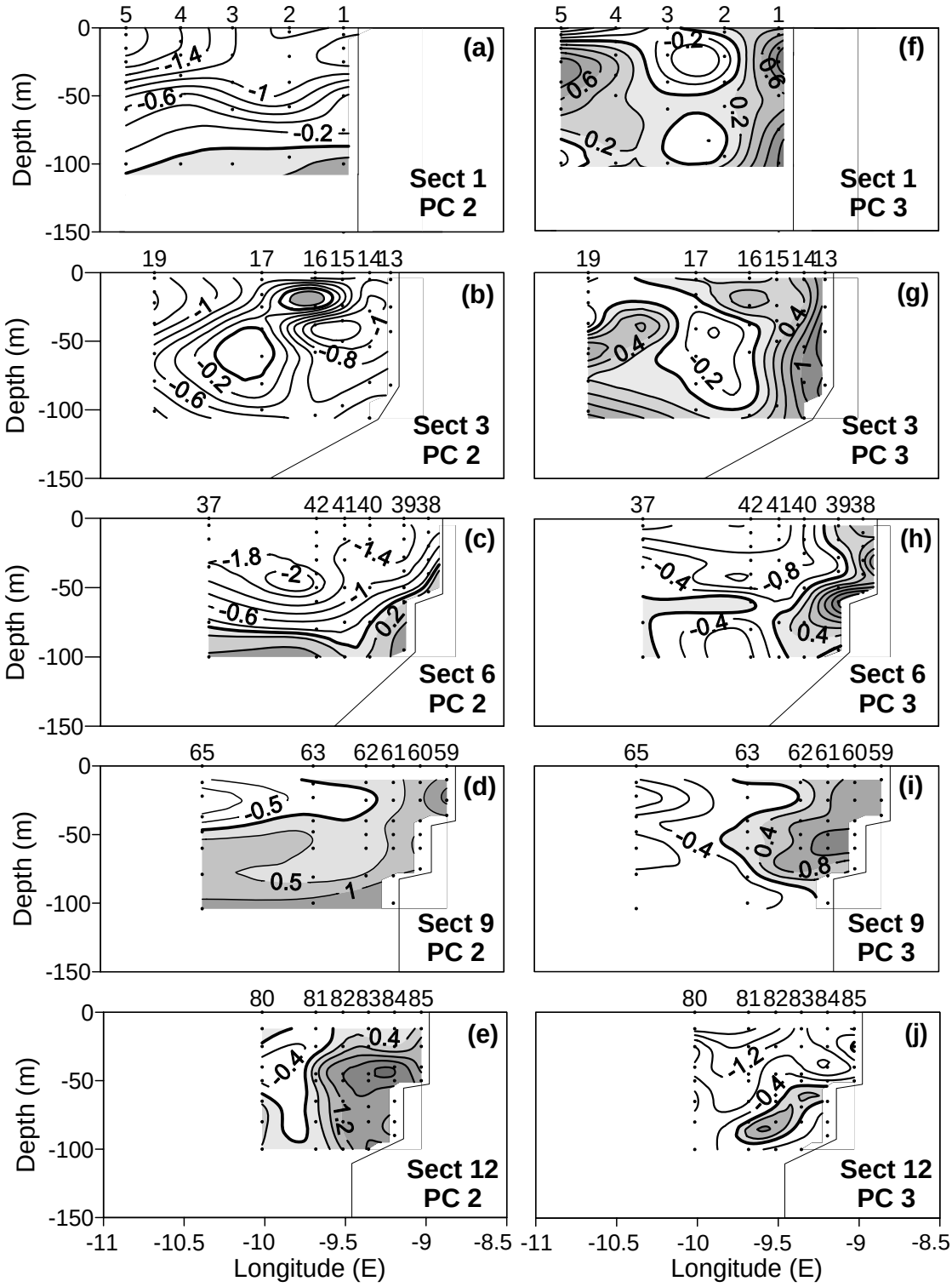

Fig. 8
Crespo & Figueiras

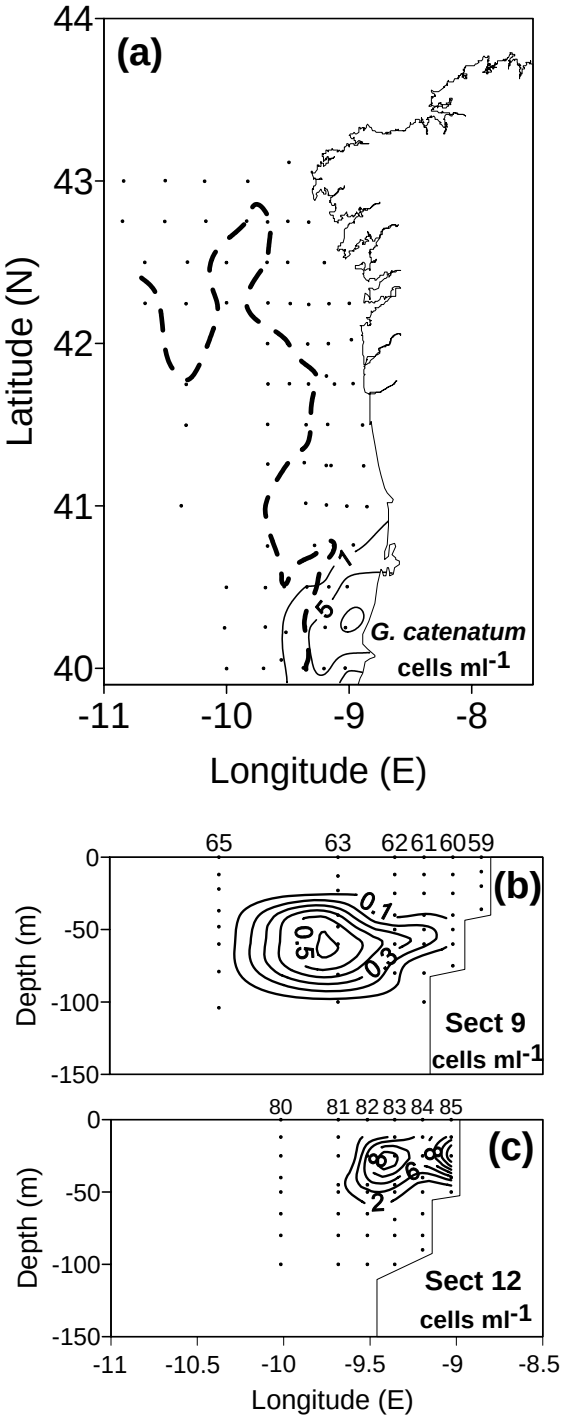

Fig. 9
Crespo & Figueiras